

# Dual emission probe for luminescence oxygen sensing: a critical comparison between intensity, lifetime and ratiometric measurements

Hannes Hochreiner, Israel Sánchez-Barragán, José M. Costa-Fernández, Alfredo Sanz-Medel\*

*Department of Physical and Analytical Chemistry, University of Oviedo, c/Julián Clavería 8, 33006 Oviedo, Spain*

Received 15 April 2004; received in revised form 2 September 2004; accepted 1 December 2004

---

## Abstract

The characterization of a dual emission sensing luminescence material for water-dissolved oxygen sensing is presented in this paper. The oxygen-sensitive material is based on a dual-emitting luminescent molecule immobilized onto an adequate solid support. The metal chelate formed between the 8-hydroxy-7-iodo-5-quinolinesulphonic acid (Ferron) and aluminium (Al-Ferron) was the selected oxygen-sensitive dual-emitting luminescent complex, while the anionic exchanger Dowex 1X2-200 resin was the selected solid support.

When the Al-ferron metal chelate is adsorbed onto the anionic exchanger resin it displays two largely different emission bands. The first is a fluorescence emission band, possessing a decay time in the nanosecond range, and which is insensitive to the oxygen presence (the “reference” signal). The second emission is a long-lived highly sensitive oxygen-quenchable phosphorescent emission. Under some optimised experimental conditions both emissions can be simultaneously measured when the metal chelate is excited with a 390 nm light. Under these conditions, and using the same experimental set-up, oxygen concentration can be obtained by measuring the intensity of the phosphorescent emission, the triplet lifetime of the phosphorescence emission or the ratio between the intensity of the phosphorescence emission and the self-reference signal (fluorescence emission from the immobilized metal chelate).

The reliability, the operational characteristics, the stability and the analytical performance characteristics for water-dissolved oxygen sensing are evaluated and critically compared for each measurement principle. Advantages and disadvantages of each measurement scheme for reliable optical sensing will be finally discussed.

© 2004 Elsevier B.V. All rights reserved.

**Keywords:** Oxygen sensing; Luminescence intensity; Ratiometric sensing; Luminescence lifetime; Phosphorescence; Fluorescence

---

## 1. Introduction

Concentration of dissolved oxygen in waters plays a crucial role in a wide range of biological and environmental processes. Therefore, real time sensing of dissolved oxygen has attracted a lot of scientific efforts and still remains a research topic of great importance for many different biological, clinical, environmental and industrial applications [1–3]. Particularly, a lot of attention has been dedicated to optical oxygen sensing in recent years. As compared with the most frequently employed Clark-type electrode system [4], optical

oxygen sensors offer several important advantages as they do not affect the sample, do not suffer from interferences from external electromagnetic fields and offer a great potential for remote control (by using optical fibres) and for miniaturization [5–7].

Among the different strategies proposed for oxygen optical detection, luminescence-quenching phenomena have proved to be one of the most powerful approaches; most of them are based on dynamic quenching of a luminescence indicator by oxygen in a collision process [8]. That is, the presence of the quencher (oxygen) in the luminescent system results in a rapid depletion of the excited-state population, which is detected as a concomitant decrease in the luminescence emission signal. The magnitude of the decrease determines the amount of analyte present.

---

\* Corresponding author. Tel.: +34 985 10 34 74; fax: +34 985 10 31 25.

E-mail addresses: [raelsb77@hotmail.com](mailto:raelsb77@hotmail.com) (I. Sánchez-Barragán), [asm@uniovi.es](mailto:asm@uniovi.es) (A. Sanz-Medel).

Materials with long excited-state lifetimes (such as the phosphorescent materials) will be particularly adequate to be quenched by oxygen. The effect of oxygen on the luminescence emission of such sensing materials results in high phosphorescence quenching rates and therefore it offers opportunities for highly sensitive oxygen sensors. In this case, quenching occurs by energy transfer from the luminescent material to form an excited singlet oxygen, resulting in excellent sensitivity and selectivity; therefore this principle was often adopted for the development of many oxygen optical sensors [5,9–11]. Many organic compounds (e.g. pyrene and other PAHs) and various transition metal complexes (e.g. platinum and palladium porphyrines, metal chelates of several hydroxyquinoline derivatives with some transition metals, etc.) were found to exhibit strong room temperature phosphorescence (RTP) emission and were applied to the development of RTP oxygen sensors.

Three basic ways can be used to monitor oxygen concentrations by using luminescence: intensity, lifetime and ratiometric measurements. Each of them has strengths and weaknesses.

Direct intensity measurements of the phosphorescence emission are, due to their simplicity in terms of instrumentation, still a very common measuring principle in phosphorimetry [12]. However, excited-state lifetime measurements are preferred today in terms of accuracy, since they are not so prone to errors derived from drifts in the opto-electronical set-up, leaching or photo-bleaching of the sensing material or transmission changes in the optics [13]. The resulting complexity of the equipment required for these lifetime measurements (based on pulsed or phase-modulation techniques) is, in any case, a drawback. As a third approach, efforts have been focused during the last few years to establish “ratiometric methods” based on the use of an internal reference. Lifetime and ratiometric approaches usually result in more robust sensing systems that are less affected by problems related to non-analyte induced intensity changes [14–16].

Ratiometric methods employing two different luminescent species immobilised in the same matrix [17] have been proposed. Another alternative is based on the use of two different excitation or emission wavelengths from a single luminescent indicator [14,18]. In the two-dye method, photobleaching of either dye leads to gross changes in the intensity ratio and this problem is eliminated by using a single, dual-emitter, molecule where the intensity ratio would be insensitive to photobleaching [19]. However, it is difficult to find single indicator molecules for oxygen exhibiting a spectral region easily quenched, enhanced or shifted in the presence of the analyte, while the other must be unaffected by its presence.

Previous work in our research group demonstrated that the metal chelate formed between the 8-hydroxy-7-iodo-5-quinolinesulphonic acid (Ferron) and aluminium (Al-Ferron) trapped into different solid supports constitutes an excellent oxygen indicator based on RTP quenching measurements [5,9].

In the present paper, we describe the use of this luminescent metal chelate as a dual-emitter system for studying comparatively ratiometric-based oxygen measurements. Using this sensing material it is possible by changing slightly the experimental parameters to obtain dissolved-oxygen concentrations from measurements of intensity ratios, RTP intensities or triplet-lifetimes. This allows a critical comparison of the three methodologies in terms of simplicity, cost, stability, accuracy and analytical performance characteristics for water-dissolved oxygen sensing, as described in the following sections.

## 2. Experimental

### 2.1. Reagents and solutions

Analytical reagent-grade chemicals were employed for the preparation of all the solutions. Freshly prepared ultra-pure deionised water (Milli-Q3 RO/MilliQ2 system, Millipore, UK) was used in all experiments.

8-Hydroxy-7-iodo-5-quinolinesulphonic acid (Ferron, Sigma–Aldrich) and aluminium standard solution (aluminium nitrate in nitric acid 0.5 M, 1000 mg/l Al, Merck) were used as delivered from the respective suppliers without any further purification. Ammonium acetate (p.a., Merck), acetic acid (glacial, Merck) and 1,10-phenanthroline-1-hydrate (Aldrich) were employed for preparation of the buffer solutions.

Dowex 1 × 2-200 was purchased from Aldrich and washed thoroughly with water, 2 M HCl solution and ethanol before use as described elsewhere [20].

Air and argon, both with purity higher than 99.995%, were purchased from Air Liquid (Llanera, Asturias, Spain).

### 2.2. Instrumentation

All luminescence data were collected with a Perkin-Elmer Model LS50B luminescence spectrometer. Instrument excitation and emission slits were set at 15 and 20 nm, respectively. A conventional Hellma fluorescence flow-through cell made of quartz (Model 176.052-QS) of 1.5 mm of light path was used.

The pH measurements were made with a Crison micro-pH 2000 digital pH-meter.

Dissolved oxygen determinations, as described in some experiments, were also performed using a commercial Crison Oximeter (OXI 330i) provided with a galvanic oxygen sensor (CelloX 325).

### 2.3. Preparation of the resin beads

The preparation of the oxygen sensing material was carried out as previously described in the literature [5]. A volume of 35 ml of Ferron solution ( $3 \times 10^{-3}$  M), 3 ml of Al(III) standard solution (1 g/l) and 10 ml of a 2 M

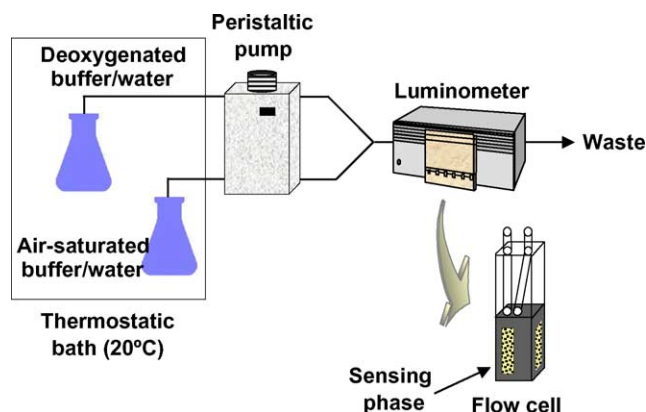


Fig. 1. Experimental set-up used for RTP dissolved-oxygen determinations.

$\text{NH}_4\text{OAc}/\text{AcOH}$  buffer solution (pH 5.5 containing 50 mg/l of 1,10-phenanthroline-1-hydrate) were mixed in a 100 ml flask and made up to the mark with Milli-Q water. The obtained Al-Ferron solution was pumped through a mini-column packed with Dowex  $1 \times 2-200$  during 30 min at a flow rate of about 2 ml/min. Later, the column was rinsed with a 1 M NaCl solution for 20 min and finally with Milli-Q water for about 10 min. The Al-Ferron immobilised resin was stored in Milli-Q water at room temperature and in the dark before use.

#### 2.4. Experimental set-up

Fig. 1 shows the optosensing device for continuous monitoring of water-dissolved oxygen. Buffer (0.5 M  $\text{NH}_4\text{OAc}/\text{AcOH}$ ; pH = 5.5, containing 50 mg/l of 1,10-phenanthroline) or water flow streams with different concentrations of dissolved oxygen were prepared by mixing varying flow rates of two streams of an air-saturated liquid and an argon-deoxygenated liquid by using two four channel Gilson Minipuls-2 peristaltic pumps. To obtain a deoxygenated solution, argon was bubbled through the solution contained in an Erlenmeyer flask. Oxygen-saturated solutions were prepared in another Erlenmeyer flask by continuously bubbling a stream of synthetic air.

Water or buffer streams, with different dissolved oxygen concentrations, were passed through a conventional flow-through cell packed with the polymeric resin particles in which Al-Ferron had been previously immobilized. A small piece of nylon was placed (away of the light path) inside the cell to prevent particles displacement and losses of the sensing material by the carrier flow. This flow-cell was placed inside the sample-holder of the phosphorimeter and luminescence emissions from the packed sensing material were continuously monitored.

To control the temperature, the flasks were immersed in a thermostatic water bath at 20 °C.

A commercial oxymeter, previously validated against the well-known Winkler method, was employed as the alternative reference method.

#### 2.5. Data acquisition

10 and 20 nm were used as excitation and emission slits widths, respectively, for all experiments. Other instrumental parameters, like the flash counts or the cycle time, proved to have no significant influence and therefore were left as set by default in the Perkin-Elmer LS50B luminometer.

For the direct RTP intensity-based measurements a delay time of 40  $\mu\text{s}$  and a gate time of 2 ms were selected. Excitation and emission wavelengths were fixed at 390 and 580 nm, respectively.

Ratiometric measurements were performed by measuring, in a fast way (at a scan speed of 600 nm/min), the total emission spectra from the sensing material (between 450 and 650 nm) under excitation at 390 nm. In these experiments the delay-time was adjusted to 30  $\mu\text{s}$  in order to allow simultaneous measurement of the phosphorescence emission in the presence of a significant fluorescence emission.

Moreover, in order to measure the triplet emission lifetimes the RTP decay curve of the sensing material should be obtained. Thus, we obtained the corresponding RTP decay curves with the proposed system by measuring the RTP intensity (at conditions previously reported for the intensity measurements) at 12 different delay times going from 40 to 100  $\mu\text{s}$ . From such averaged curves, lifetimes can be calculated because RTP intensity and lifetime are related by the equation:

$$I(t) = I(0)e^{-t/\tau} \quad (1)$$

where  $I(t)$  is the intensity for the instant of time  $t$ ,  $I(0)$  the intensity when  $t = 0$  and  $\tau$  the triplet lifetime.

### 3. Results and discussion

#### 3.1. Spectral characteristics of the oxygen sensing material

Fig. 2 shows the emission luminescence spectra of the immobilized Al-Ferron chelate exposed to a deoxygenated buffer stream at different delay times. The gate time was set at a value of 1.0 ms. As can be seen, the excitation spectrum has a maximum centred in 395 nm, while, depending on the delay time, it is possible to clearly distinguish simultaneously two emission bands centred at 470 and 580 nm.

The first emission band corresponds to a fluorescence emission ( $\lambda_{\text{em}} = 470 \text{ nm}$ ) that still remains even at a delay time of 30  $\mu\text{s}$ . As can be seen this emission band decreases drastically with increasing the delay time, and practically disappears for a delay time of 40  $\mu\text{s}$ . However, for delay times lower than 30  $\mu\text{s}$  the fluorescence band highly increases and completely overlaps with the second emission band (being not possible to simultaneously measure both emission signals in such conditions).

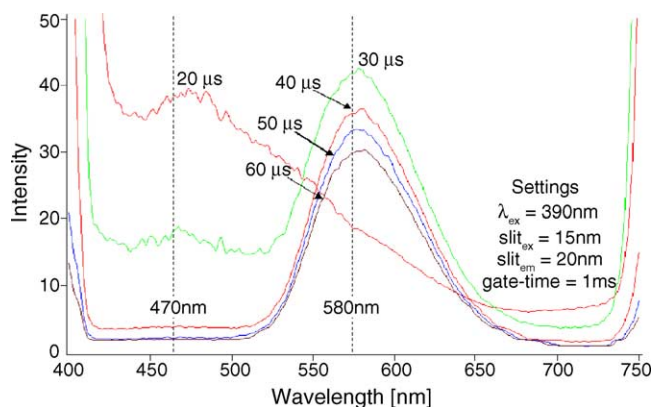


Fig. 2. Emission spectra of the oxygen sensing material obtained at different delay times (20, 30, 40, 50  $\mu$ s) when exposed to a deoxygenated buffer stream. (Note: the intensity values of the emission spectra for  $t_d = 20 \mu$ s should be multiplied by a factor of 5).

The second emission band (centred at 580 nm) is a phosphorescence emission. This band has a rather longer lifetime as compared to the fluorescence emission (the intensity decrease with the increase on the delay time is much slower as compared to the fluorescence band).

Fig. 3 shows the emission luminescence spectra of the immobilized Al-Ferron chelate, exposed to buffer streams with different dissolved oxygen concentrations. In order to allow for the simultaneous measurement of both fluorescence and phosphorescence emission the luminometer was set at a delay time of 30  $\mu$ s and at 1.0 ms gate time. As can be seen in Fig. 3, the fluorescence emission does not suffer any appreciable changes with oxygen concentration (even if dissolved oxygen concentration is increased up to saturation levels). However, the emission at 595 nm (corresponding to the phosphorescence emission) is strongly quenched by the presence of oxygen. This makes this Al-Ferron luminescence indicator specially suited not only for phosphorimetric (intensities or lifetimes-based measurements) but also for oxygen ratiometric measurements.

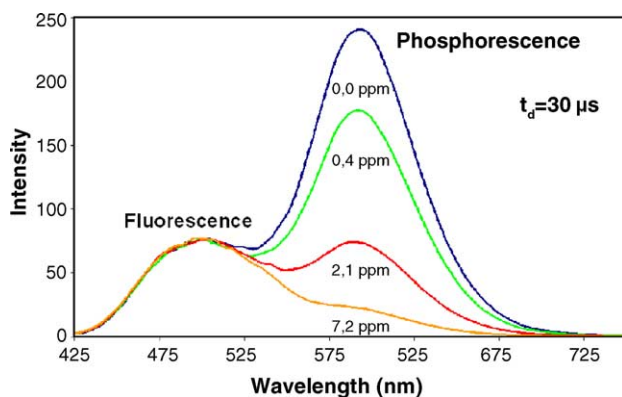


Fig. 3. Emission spectra of the oxygen sensing material obtained when exposed to buffer streams containing 0.0, 0.4, 2.1 and 7.2 ppm of dissolved oxygen.

Table 1

Effect of variations on the slit widths on the luminescence measurements from the oxygen sensing material (in the presence of a deoxygenated buffer stream)

Measurement method	Slit widths (excitation/emission) (nm)					
	10/20	15/20	5/20	10/10	10/5	10/15
Intensity emission (a.u.)	149.4	115.2	158.6	44.0	8.3	101.5
Ratiometric measurements	2.5	2.5	2.2	2.4	2.3	2.5
Lifetimes ( $\mu$ s)	56.5	56.5	58.6	55.9	56.4	56.7

### 3.2. Effect of instrumental and environmental variations on the luminescence signals

As shown before, both the RTP intensity and triplet lifetime of the trapped RTP chelate decreased in the presence of oxygen, while fluorescence is not affected by oxygen presence. Thus, we could use RTP intensity, triplet lifetime or ratiometric measurements to obtain the actual oxygen concentration in three different ways. Thus, we studied the effect on the sensing performance of variations in several instrumental, physico-chemical and active phase parameters (which could affect the luminescence measurements and so affecting the measured oxygen concentrations). To do that, different parameters were slightly modified and the potential changes in the RTP intensity emission, ratiometric measurement and excited lifetime values from the sensing material (in the presence of a deoxygenated buffer stream) were registered.

First, the effect of changes in excitation and emission slits width on the emission signals from the sensing material was studied. Results are summarised in Table 1. As can be seen, while RTP intensity emission signals were highly influenced by variations on the slits width (changes on the emission signals over 60% have been found), ratiometric and lifetime measurements were not significantly affected by those changes (variations in the signals only of about 5 and 2% have been found for ratiometric and lifetime measurements, respectively).

A study of the effect on the RTP signals of variations of the indicator concentration in the light path were also made by changing the particle size packed in the flow cell. From this study it was observed that both, ratiometric measurements and RTP lifetime values from the sensing material, are not significantly affected by alterations on the solid particles size. However, as expected, important variations of the RTP intensities were observed depending on the size of the sensing particles.

A special care should be taken with changes in temperature. We have studied here the effect of sample temperature on the measured RTP signals, as previous experiments carried out in our lab demonstrated great temperature influence on the RTP intensity and lifetime measurements. Temperature increases gave rise to a significant decrease of the measured signals (intensity and lifetimes) and consequently erroneous determinations were observed. For a given dissolved oxygen concentration, a linear relationship was found between the

measured RTP signals and the sample temperature (it was observed that a temperature variation of 10 °C resulted in a 10% deviation of the phosphorescence emission at 20 °C). Similarly, the fluorescence emission was also significantly quenched by a temperature increase, but with a different behaviour as compared to the RTP. This would be reflected in the ratiometric measurements. In fact, it was observed that, for a given dissolved oxygen concentration, a temperature increase resulted in a decrease in the measured  $I_{\text{RTP}}/I_{\text{F}}$  ratio. A lineal dependence between temperature and the ratiometric measurement was found (in this case, a temperature variation of 10 °C resulted in a 8% deviation of the measured  $I_{\text{RTP}}/I_{\text{F}}$  ratio at 20 °C). Therefore, a correction of the luminescence signals with temperature (or calibrations of the sensing probe with standards at the same temperature of the samples) should be carried out. Thus, all the experiments were conducted at a controlled samples temperature (20 °C), something easily achieved by using a thermostatic water bath.

When using the sensor for oxygen determinations in aqueous solutions, variations in pH between 3 and 8 caused small variations in the luminescence signals from the immobilized metal chelate being the optimum value pH = 5.5. Therefore, most of the optimizations and experiments were carried out using a 0.5 M  $\text{NH}_4\text{OAc}/\text{AcOH}$  buffer of pH 5.5.

The potential interferent effect of calcium ions (up to 600 ppm) and other metal ions including  $\text{Pb}^{+2}$ ,  $\text{Fe}^{3+}$  and  $\text{Hg}^{+2}$  (up to 10 ppm) was studied. It was found that only small concentrations of Fe(III) caused a severe interference by chemical decomposition of the phosphorescent probe, although this interference was avoided by adding 1,10-phenanthroline to every buffer and carrier solutions.

Finally, the influence of ionic strength on the luminescence signals from the oxygen sensing phase was evaluated. The phosphorescence emission and the ratiometric measurements from the sensing material were registered when exposed to deoxygenated water solutions with increasing concentrations of different electrolytes ( $\text{NaCl}$ ,  $\text{KCl}$  and  $\text{BaCl}_2$ ) up to an ionic strength of 0.1 M. As expected, changes in the luminescence emission with ionic strength increase were found to be similar for all evaluated salts. On the other hand, it was found that ratiometric measurements offer slightly better reliability as compared with phosphorescence intensity measurements (variations of the signal with the ionic strength up to 7–8% were obtained for direct RTP measurements while variations below 4% were found using ratiometric measurements).

### 3.3. Quenching measurements for water-dissolved oxygen sensing

It was observed that the RTP emission of the Al-Ferron metal chelate immobilized onto the anionic exchange resin matrix is reversibly quenched when exposed to on–off cycles of dissolved oxygen. Moreover, no appreciable leaching of the immobilized indicator was observed even after more than 48 h of continuous use. As it is possible to make use of RTP intensities, triplet lifetimes or ratiometric lumines-

cence emission measurements from this sensing material to perform oxygen determinations, the performance of the different luminescence measurement approaches was evaluated for reliable oxygen sensing.

First, the variability of the corresponding calibration-plots of this luminescent oxygen sensor was evaluated in several different days. This would be an indicator of the reliability and stability of each of the sensing approaches. To do that, five different dissolved oxygen calibration plots were obtained along five different days for each one of the measurement principles using the proposed optosensing system and the obtained results were compared.

For establishing those calibration curves the obtained data were fitted to the well known Stern–Volmer Eq. (2) commonly used in luminescence-quenching methods:

$$\frac{\tau_0}{\tau} = \frac{I_0}{I} = 1 + k_2\tau_0[Q] = 1 + K_{\text{SV}}[Q] \quad (2)$$

where  $\tau_0$  or  $I_0$  and  $\tau$  or  $I$  denote the luminescence lifetime or intensities of the luminophor in the absence and in the presence of a quencher, respectively,  $k_2$  and  $K_{\text{SV}}$  are the bimolecular quenching and the Stern–Volmer constants and  $Q$  the concentration of the quencher. This form of the Stern–Volmer equation represents the simplest approach and only accounts for purely dynamic quenching of one luminescent species in a homogeneous environment.

Lifetime data showed very good agreement to this version of the equation and the linear graphs were obtained and used for sensor calibration. However, for intensity and ratiometric measurements, clearly non-linear Stern–Volmer plots (positive deviation from linearity) were obtained. Similar findings were previously reported by other authors and different models (modifications of the Stern–Volmer equation) were proposed trying to explain these deviations based on multi-site models or multi-exponential decays [21–24]. Unfortunately none of these models could explain the positive deviations from the Stern–Volmer plot found in our experiments.

Of special interest is the model proposed when both, static and dynamic quenching, occur in the same system [25,26], a model explaining positive deviations from linearity in the simple Stern–Volmer plot. The co-existence of dynamic and static quenching caused by oxygen has been recently described by Hurtubise et al. [27] and Gillanders et al. [28]. The following modified Stern–Volmer plot should then be used when static and dynamic quenching occur simultaneously:

$$\frac{I_0}{I} = 1 + (K_{\text{SV}} + K_{\text{eq}})[Q] + K_{\text{SV}}K_{\text{eq}}[Q]^2 \quad (3)$$

This modified Eq. (3) was used in our experiments and a better fit of the experimental data was obtained using both RTP intensities and ratiometric measurements.

Table 2 summarises the calibration functions obtained along 5 days using the three sensing approaches based on the different measurement principles. As can be seen, some differences in the calibration plots can be observed along the five

Table 2

Summary of the calibration functions for the different measurement methods obtained through five different days

	Intensity measurements	Ratiometric measurements	Lifetime measurements
Day 1	$(I_0/I) - 1 = 0.1540[\text{O}_2]^2 + 0.7290[\text{O}_2]$	$[(I_{\text{RTP}}/I_F)_0/(I_{\text{RTP}}/I_F) - 1 = 0.0457[\text{O}_2]^2 + 0.6771[\text{O}_2]$	$(\tau_0/\tau) - 1 = 0.4054[\text{O}_2]$
Day 2	$(I_0/I) - 1 = 0.1778[\text{O}_2]^2 + 0.5940[\text{O}_2]$	$[(I_{\text{RTP}}/I_F)_0/(I_{\text{RTP}}/I_F) - 1 = 0.0594[\text{O}_2]^2 + 0.6981[\text{O}_2]$	$(\tau_0/\tau) - 1 = 0.4291[\text{O}_2]$
Day 3	$(I_0/I) - 1 = 0.1546[\text{O}_2]^2 + 0.8275[\text{O}_2]$	$[(I_{\text{RTP}}/I_F)_0/(I_{\text{RTP}}/I_F) - 1 = 0.0495[\text{O}_2]^2 + 0.7838[\text{O}_2]$	$(\tau_0/\tau) - 1 = 0.4219[\text{O}_2]$
Day 4	$(I_0/I) - 1 = 0.2132[\text{O}_2]^2 + 1.1167[\text{O}_2]$	$[(I_{\text{RTP}}/I_F)_0/(I_{\text{RTP}}/I_F) - 1 = 0.0476[\text{O}_2]^2 + 1.0198[\text{O}_2]$	$(\tau_0/\tau) - 1 = 0.5438[\text{O}_2]$
Day 5	$(I_0/I) - 1 = 0.1766[\text{O}_2]^2 + 0.9621[\text{O}_2]$	$[(I_{\text{RTP}}/I_F)_0/(I_{\text{RTP}}/I_F) - 1 = 0.0506[\text{O}_2]^2 + 0.8240[\text{O}_2]$	$(\tau_0/\tau) - 1 = 0.4402[\text{O}_2]$

different days. However, it is apparent that great differences between the five calibration plots are observed using intensity measurements (deviations in the slope values of about 20% can be found) while triplet lifetimes or ratiometric measurements provided lower deviations in the slope values of the plots (average of about 12%).

In a next step, the three different RTP measurement approaches were applied to the analysis of several water samples. The water-dissolved oxygen concentrations were then obtained from the measured luminescence values and using the different calibration plots (performed during the five different days). The obtained results were compared to the values given by a reference method (commercial oxymeter previously validated with a classical Winkler method) in each case and sample.

Fig. 4 shows the relative errors (%) found in the oxygen determinations with each of the three methods under scrutiny and using the different calibration plots. As can be seen, ratiometric measurements outperform the other two approaches in terms of reliability of the measurement method. Moreover, as expected, the greatest differences between the results obtained by interpolation of the analytical signals in calibration plots from different days were found for phosphorescence intensity-based measurements. Thus, the need for a daily calibration when using intensity measurements is clearly patent.

### 3.4. Analytical performance of the different approaches for dissolved oxygen sensing

The analytical figures of merit for the different sensing approaches (using the different measurement principles) are summarised in Table 3. Calibration graphs were obtained from the luminescence signals from the sensing material when exposed to aqueous solutions of increasing dissolved-oxygen concentrations (confirmed by simultaneous measurement of the dissolved oxygen concentrations with the reference electrochemical oxymeter). The Stern–Volmer plots (or their modified forms) were obtained

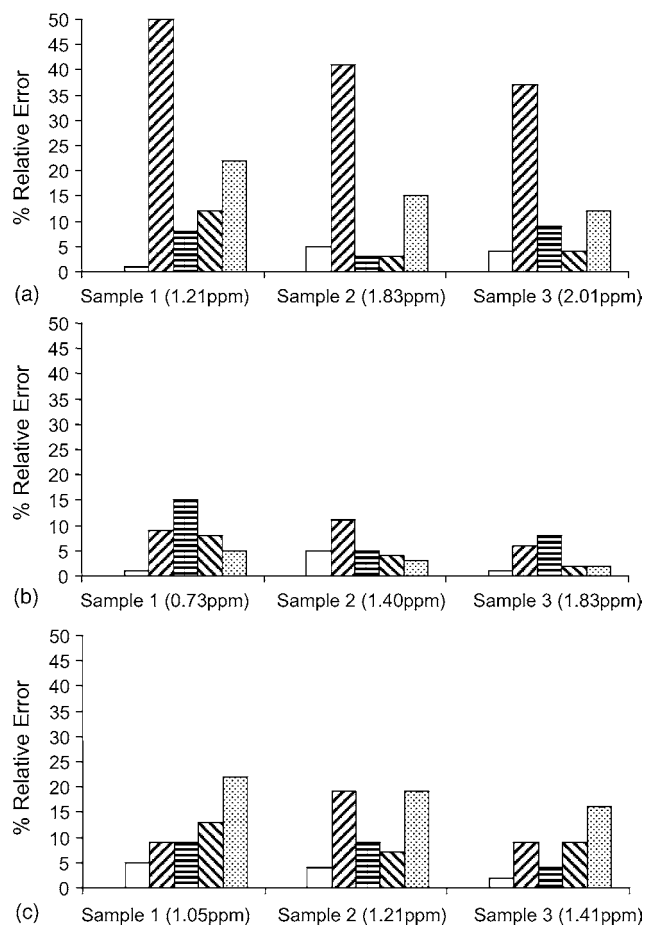


Fig. 4. Dissolved oxygen sensing of different water samples using (a) intensity measurements, (b) ratiometric measurements and (c) lifetime measurements. Day 1 samples refer to sample measurements made on the same day as the calibration; (□) day 1, (▨) day 2, (≡) day 3, (≡) day 4, (⊞) day 5.

and yielded a good regression coefficient in every case up to oxygen saturation levels.

The repeatability of the proposed sensing approaches was evaluated as the relative standard deviation of five replicates

Table 3

Analytical figures of merit for dissolved oxygen measurement using the different optosensing approaches

	Intensity measurements	Ratiometric measurements	Lifetime measurements
Calibration range (ppm)	0.06–7.24	0.30–7.24	0.06–7.24
Limit of detection (ppm)	0.02	0.10	0.02
Repeatability (R.S.D.) (%)	3	4	1
Precision (R.S.D.) (%)	16	5	7

of a sample containing 1 ppm of dissolved oxygen measured along a single experiment in the same day and under the same experimental conditions. The detection limits were calculated as the minimum concentration of dissolved oxygen detectable (which produced an analytical signal three times the standard deviation of the blank signal, IUPAC criterion). As can be seen in Table 3, lifetime measurements still show the best average values in terms of reproducibility and limits of detection. While the limit of detection with ratiometric measurements was a little bit worse than using intensity measurements, the performance of the two methods in terms of reproducibility is less comparable.

The greatest differences between the different methods tested here can be found when comparing the precision data. Precision values were evaluated as the relative standard deviation of five measurements of a given sample with a 2 ppm oxygen concentration carried out in five different days and without performing new calibrations of the sensing system. In this case, intensity measurements yielded the worst results (%R.S.D. of the performed measurements of about 16%), while the other two measurement methods proved to be more reliable. It was found that ratiometric measurements offer slightly better precision values even compared with lifetime measurements (see Table 3). The reliability of ratiometric-based measurements, which not only show clear advantages over intensity but even over employing lifetime measurements, is impressively reflected by the accuracy of the sample measurements (see Fig. 4).

#### 4. Conclusions

The metal complex (Al-Ferron) immobilized onto a Dowex 1  $\times$  2-200 polymeric resin has demonstrated to show a dual-emission luminescence: an oxygen-non-dependent phosphorescent emission and a second oxygen-quenchable phosphorescent emission, with rather long triplet lifetimes. Thus, three RTP different methods for dissolved-oxygen sensing (based on intensity, lifetime or ratiometric measurements) can be applied by using such sensing RTP active phase.

Changes in the phosphorescence emission intensities from the sensing material with the oxygen concentration were observed to be significantly greater than the corresponding triplet-lifetime variations. Moreover, upward deviations from linearity in the simple Stern–Volmer plots were found by intensity and ratiometric measurements at high dissolved oxygen concentrations (while when using triplet lifetime measurements, the Stern–Volmer plots were found to be linear up to dissolved oxygen saturation levels). These results suggest that both static and dynamic quenching from oxygen is present in the employed RTP sensing phase (this possibility should be considered in the design of the calibration plots).

A critical comparison of the analytical performance of the three different luminescence measurement approaches under scrutiny for water-dissolved oxygen sensing has been

performed. Unlike intensity measurements, both lifetime and ratiometric measurements proved no significant dependence upon instrumental variations. Moreover, the results obtained showed that the precision and repeatability of the sensing approaches were similar using triplet lifetimes and ratiometric measurements. Those modes considerably improved the performance obtained from intensity-based measurements.

However, although lifetime and ratiometric approaches showed similar analytical performances, the ratiometric approach might be preferable because lifetime measurement usually requires a more complex instrumentation.

#### Acknowledgements

Financial support from Fundación para el Fomento en Asturias de la Investigación Científica Aplicada y la Tecnología (FICYT) through the project PC-CIS01-13 and from the projects BQU-2003-04671 and MAT2003-09074-C02 (Feder Programme and Ministerio de Ciencia y Tecnología, Spain) is gratefully acknowledged.

H. Hochreiner would like to express his gratitude to the Austrian Federal Ministry for Education, Science and Culture (Stipendien für kurzfristige wissenschaftliche Arbeiten und den Besuch fachspezifischer Kurse im Ausland) for an Erasmus Grant.

#### References

- [1] M. Radojevic, V.N. Bashkin, *Roy. Soc. Chem.* (1) (1999).
- [2] O.S. Wolfbeis, *Anal. Chem.* 72 (2000) R81–R89.
- [3] M. Stücker, L. Schulze, G. Pott, P. Hartmann, D.W. Lübbers, A. Röchling, P. Altmeyer, *Sens. Actuat. B* 51 (1998) 171–175.
- [4] O.S. Wolfbeis, *Fiber Optic Chemical Sensors and Biosensors*, vol. 1, CRC Press, Boca Ratón, 1991.
- [5] J.M. Costa-Fernández, M.E. Díaz-García, A. Sanz-Medel, *Anal. Chim. Acta* 360 (1998) 17–26.
- [6] J. Lin, *Trends Anal. Chem.* 19 (2000) 541–552.
- [7] O.S. Wolfbeis, *Anal. Chem.* 74 (2002) 2663–2678.
- [8] J.N. Demas, B.A. DeGraff, P.B. Coleman, *Anal. Chem.* 71 (1999) 793A–800A.
- [9] Y.M. Liu, R. Pereiro-García, M.J. Valencia-González, M.E. Díaz-García, A. Sanz-Medel, *Anal. Chem.* 66 (1994) 836–840.
- [10] J.M. Costa Fernández, A. Sanz-Medel, *Química Analítica* 19 (2000) 189–204.
- [11] J. Kuijt, F. Ariese, U.A.T. Brinkman, C. Gooijer, *Anal. Chim. Acta* 488 (2003) 135–171.
- [12] Y. Liu, R. Pereiro García, M.E. Díaz García, A. Sanz-Medel, *Anal. Chim. Acta* 255 (1991) 245–251.
- [13] V.I. Ogurtsov, D.B. Papkovsky, *Sens. Actuat. B* 51 (1998) 377–381.
- [14] Y. Kostov, K.A. Van Houten, P. Harms, R.S. Pilato, G. Rao, *Appl. Spectrosc.* 54 (2000) 864–868.
- [15] Y. Kostov, P. Harms, R.S. Pilato, G. Rao, *Analyst* 125 (2000) 1175–1178.
- [16] A. Song, S. Parus, R. Kopelman, *Anal. Chem.* 69 (1997) 863–867.
- [17] H.M. Rowe, S.P. Chan, J.N. Demas, B.A. DeGraff, *Appl. Spectrosc.* 57 (2003) 532–537.
- [18] Y. Kostov, G. Rao, *Sens. Actuat. B* 90 (2003) 139–142.
- [19] S.L.R. Barker, H.A. Clark, S.F. Swallen, R. Kopelman, A.W. Tsang, J.A. Swanson, *Anal. Chem.* 71 (1999) 1767–1772.

- [20] J.M. Costa-Fernández, A. Sanz-Medel, M.E. Díaz-García, *Sens. Actuat. B* 38 (1997) 103–109.
- [21] P.Y.F. Li, R. Narayanaswamy, *Analyst* 114 (1989) 1191–1195.
- [22] P. Hartmann, M.J.P. Leiner, M.E. Lippitsch, *Anal. Chem.* 67 (1995) 88–93.
- [23] A. Mills, *Sens. Actuat. B* 51 (1998) 69–76.
- [24] H. Shiroishi, K. Suzuki, M. Seo, S. Tokita, M. Kaneko, *J. Comp. Sci. Jpn.* 1 (2002) 37–46.
- [25] W. Xu, R. Schmidt, M. Whaley, J.N. Demas, B.A. DeGraff, E.K. Karikari, B.L. Farmer, *Anal. Chem.* 67 (1995) 3172–3180.
- [26] L.A. Sacksteder, J.N. Demas, B.A. DeGraff, *Anal. Chem.* 65 (1993) 3480–3483.
- [27] R.J. Hurtubise, A.H. Ackerman, B.W. Smith, *Appl. Spectrosc.* 55 (2001) 490–495.
- [28] R.N. Gillanders, M.C. Tedford, P.J. Crilly, R.T. Bailey, *J. Photochem. Photobiol.* 163 (2004) 193–199.